

# EEG Microstate in Obstructive Sleep Apnea Patients

**Xin Xiong**

Kunming University of Science and Technology

**Yuyan Ren**

Kunming University of Science and Technology

**Shenghan Gao**

Kunming University of Science and Technology

**Jianhua Luo**

Kunming University of Science and Technology

**Jiangli Liao**

Kunming University of Science and Technology

**Chunwu Wang**

Jilin Normal University

**Sanli Yi**

Kunming University of Science and Technology

**Ruixiang Liu**

Second People's Hospital of Yunnan Province

**Yan Xiang**

Kunming University of Science and Technology

**Jianfeng He** (✉ [jfenghe@foxmail.com](mailto:jfenghe@foxmail.com))

Faculty of Information Engineering and Automation, Kunming University of Science and Technology, Kunming, 650500, China;

---

## Research Article

**Keywords:** Obstructive sleep apnea (OSA), electroencephalogram (EEG), detrended fluctuation analysis (DFA)

**Posted Date:** December 9th, 2020

**DOI:** <https://doi.org/10.21203/rs.3.rs-120777/v1>

**License:** © ⓘ This work is licensed under a Creative Commons Attribution 4.0 International License. [Read Full License](#)

---

# Abstract

Obstructive sleep apnea (OSA) is a common sleep respiratory disease. Previous studies have found that the wakefulness electroencephalogram (EEG) of OSA patients has changed, such as increased EEG power. However, whether the microstate reflecting the transient state of the brain is abnormal is unclear during sleep apnea or hypopnea. We investigated the microstates of sleep EEG in 30 OSA patients and in 10 healthy control volunteers. Then correlation analysis was carried out between microstate parameters and EEG markers of sleep disturbance, such as power spectrum, sample entropy and detrended fluctuation analysis (DFA). We observed that there was an additional fifth microstate E during apnea or hypopnea in N1 and N3 stages in OSA patients. And the microstate E was correlated with the power spectrum of delta, theta and alpha bands, not correlated with sample entropy, but correlated with DFA in N1-OA/OH stage. Moreover, Global Explained Variance, Mean Duration, Time Coverage and Segment Density of microstate E were positively correlated with DFA. We can interpret that the abnormal transition of brain active areas of OSA patients in N1-OA/OH stages leads to an extra microstate E, which might be related to the change of alpha activity in the cortex. And the generation of microstate E is not correlated with the decrease of EEG complexity, but correlated with the stronger self-similar regularity of EEG signals in OSA patients. These findings indicate that the microstate has the potential as a biomarker of EEG and has potential application value in OSA diagnosis.

## Introduction

Obstructive sleep apnea (OSA) is a common sleep disorder. With the increase of obesity rate, its prevalence is also increasing<sup>1</sup>. It is a chronic multisystem disease, which may lead to a variety of acute clinical problems at the same time, including hypertension, cardio cerebral stroke, mechanical infarction, etc.<sup>2</sup> OSA causes repeated airflow interruption and/or reduction due to stenosis of the upper airway during sleep, resulting in fragmentation of sleep and hypoxemia<sup>3</sup>. These affect the neurobehavioral function of OSA patients, for example, the risk of car accident in OSA patients increases by 2–10 times<sup>4</sup>.

Despite the prevalence of OSA, its underlying neurophysiological process is unclear. Current research results all support that its pathogenesis is multifactorial, such as oxidative stress leading to vascular endothelial cell damage and atherosclerosis, which is related to cardiovascular and cerebrovascular diseases, metabolic diseases, sudden death and other multi-system damage. The damage also aggravates OSA, forming a vicious circle and disease progression. Clinical studies have shown that the EEG of OSA patients has changed, such as changes in power spectrum and energy<sup>5,6</sup>. Zhou et al. found that the sample entropy of sleep apnea syndrome patients was lower than healthy controls in each sleep stage<sup>7</sup>. Grenèche et al. found that the power of wakefulness EEG in OSA patients after 24 hours of sleep deprivation was higher than healthy controls<sup>8</sup>. D’Rozario et al. found that the wakefulness EEG power spectrum and detrended fluctuation analysis (DFA) of OSA patients were related to simulated driving performance, and the scale index  $\alpha$  of DFA can be used as an indicator of simulated driving performance<sup>9,10</sup>. Kim et al. used DFA to analyze the sleep onset period (SOP) of narcolepsy patients, and found that the SOP of narcolepsy patients was significantly larger compared with healthy controls<sup>11</sup>.

These studies provide a window for us to understand OSA patients' EEG. However, such studies are relatively few and focus on the difference of neurobehavioral ability (such as simulated driving) of OSA patients and healthy subjects<sup>8, 9, 10</sup>. To the best of our knowledge, there have been no reports of studying the EEG of OSA patients from the perspective of microstate. EEG microstate employs the information of the entire time and space of EEG to characterize the rapid spontaneous change of scalp potential with time<sup>12</sup>. Such this approach can provide a more informative framework and global interpretability without any type of a priori hypothesis<sup>13</sup>, in contrast with other EEG analysis techniques, which evaluate the brain's electrical field in a specific location (for example by a priori choice of electrodes of interest) or at determinate time intervals or in specific frequency bands<sup>14</sup>. According to the microstate theory, EEG signals are composed of a series of topographic maps with two remarkable properties<sup>12, 15</sup>: (1) EEG signals are composed of a large number of topographic maps, but most EEG signals can be expressed with a small amount of topographic maps; (2) before the transition from one topographic map to another, a single topographic map dominates with a duration of about 80 to 120 milliseconds. These metastable states are microstates, which are described as the basic components or "thought atoms" of human information processing. Therefore, the microstate analysis method is more used to study human's cognition and thinking, as well as psychotic disorders<sup>15</sup>. However, few researchers use it to study sleep, only the healthy subjects' and narcolepsy patients' sleep<sup>16, 17</sup>. Brodbeck et al. found that healthy subjects had 4 microstates during the wakefulness and NREM sleep stages<sup>16</sup>. Kuhn et al. found that narcoleptic patients in early NREM sleep had an additional microstate E during the N3 phase<sup>17</sup>. Dose the microstates of EEG in OSA patients change? If the microstates change, is there any correlation between microstate parameters and EEG markers such as power spectrum<sup>5, 6, 8, 9</sup>, sample entropy<sup>7, 18</sup>, and DFA<sup>9, 10, 11</sup>?

Therefore, we hypothesized that there were abnormal microstates in OSA patients during sleep obstructive apnea or obstructive hypopnea, and the microstate parameters were correlated with power spectrum, sample entropy and DFA.

## Results

### OSA of sleep stages

OSA may occur at any time in the sleep cycle, and the number of OH/OA occurrences in 4 sleep stages in 30 OSA patients in Subgroup\_I was counted, as shown in Table 1. OH/OA occurs more frequently in N1, N2 and R stages, less in N3 stage, and least in W stages in Table 1. Patients with more OH/OA in N1 and N2 stages also have more OH/OA in R stages, such as Sub61 and Sub80. However, patients with more OH/OA in R stages may not have more OH/OA in N1 and N2 stages, such as Sub45, Sub73, Sub87, Sub96, and Sub97.

Table 1

The number of OSA occurrences during each sleep stage of 30 OSA patients

Patient ID	Number of OSA occurrences during each sleep stage				
	W-OH/OA	N1-OH/OA	N2-OH/OA	N3-OH/OA	R-OH/OA
Sub13	7	50	4	0	0
Sub15	1	8	13	14	3
Sub16	2	31	6	3	8
Sub17	0	16	23	9	13
Sub18	0	8	5	3	0
Sub21	0	41	35	0	0
Sub33	0	1	17	0	7
Sub37	0	23	18	0	4
Sub39	0	3	0	0	10
Sub45	0	6	6	1	43
Sub53	0	0	0	0	0
Sub58	0	4	0	0	9
Sub59	0	0	0	0	15
Sub61	0	34	51	5	52
Sub69	0	0	7	1	18
Sub72	0	1	1	0	0
Sub73	0	14	10	2	52
Sub74	0	12	16	0	31
Sub77	0	13	12	11	9
Sub78	0	1	2	0	2
Sub79	0	11	10	2	0
Sub80	3	66	54	1	49
Sub81	0	6	20	0	4
Sub87	0	3	7	0	56
Sub89	1	12	50	4	14
Sub90	0	2	0	0	11
Sub91	0	3	2	2	14

Patient ID	Number of OSA occurrences during each sleep stage				
	W-OH/OA	N1-OH/OA	N2-OH/OA	N3-OH/OA	R-OH/OA
Sub96	1	2	9	0	48
Sub97	1	13	7	6	29
Sub99	0	0	0	0	7
Sub100	0	12	11	0	9
Total	16	396	396	63	517

## OSA Microstates

The microstate parameters of two groups are shown in Figs. 1 ~ 3 and Tables 2 ~ 3, and the p-value corresponding to the independent sample *t* test is performed. Because there were additional microstates E in N1-OH/OA and N3-OH/OA stages in OSA patients, and there was no corresponding microstate in healthy controls, microstate E did not participate in independent sample *t* test. The statistical results showed that except for Mean Duration of microstate C and D in N1-OH/OA stage ( $p = 0.029$ ;  $p = 0.033$ ) and Mean Duration of microstate D in N3-OH/OA stage ( $p = 0.038$ ) and Global Explained Variance of microstate A in R stage ( $p = 0.028$ ), there was no significant difference in the remaining microstates.

The healthy controls have four similar microstates A, B, C and D in N1, N2, N3 and R stages (ignoring the polarity of microstates<sup>19,20</sup>, as shown in Fig. 1, which is similar to the previously reported microstate of sleep EEG<sup>16,17</sup>. The microstates of OSA patients are shown in Fig. 2. It could be seen that there are four microstates similar to normal sleep stages, but the fifth microstate E (ignoring the polarity of microstate) appears in N1 and N3 stages. After fitting the microstates A, B, C, D and E back to the original EEG data, the microstate E only exists in N1-OH/OA of sub13, sub18, sub21, sub39, sub61 and sub77, and N3-OH/OA of sub15, sub16 and sub17.

The calculated microstate parameters include: Global Explained Variance (GEV), Mean Duration (MeanDur), Time Coverage (TimeCov), Segment Density (SegDensity) and Transition Probability (TP), as shown in Table 2 ~ 3 and Fig. 3.

As can be seen from Tables 2 ~ 3, GEV of the microstates A, B, C and D in OSA patients is between 22.8%~26.0%, and GEV of microstate E is relatively low, only 2.3%~2.5%. The MeanDur of microstates A, B, C and D is about 100 ~ 118 ms, while that of microstate E is 22.2 ~ 22.3 ms. Similarly, TimeCov and SegDensity of microstates A, B, C and D are between 22.2 ~ 27.8%, respectively, while those of microstate E are 2.3%~2.9%. This shows that microstate E appears for a shorter time and accounts for a lower proportion of EEG signals.

Except for extra microstate E in N1-OH/OA phase, MeanDur of microstates C and D in OSA patients are longer than healthy controls (OSA vs. Control:  $118.5 \pm 38.9$  vs.  $110.0 \pm 30.0$ ;  $112.6 \pm 41.2$  vs.  $100.0 \pm 0.0$ ). And MeanDur of microstate D in OSA patients was also longer than healthy controls in N3-OH/OA phase (OSA vs. control:  $118.1 \pm 47.4$  vs.  $100.0 \pm 0.0$ ).

From Fig. 3, in N1/N1-OH/OA stage, the transition probability of microstate C and D in healthy controls is higher, while that of microstate A, B and E of OSA patients is higher, and the probability of transition from microstate C to E in OSA patients is the smallest. In N2/N2-OH/OA stage, most of the curves in two groups coincided, and the probability of transition from microstate B to C in healthy controls was the lowest, while that in OSA patients was the largest. In N3/N3-OH/OA stage, the transition probability of microstate B, C and D in healthy controls was higher, while the transition probability of microstate C, D and E in OSA patients was higher, and the probability of transition from microstate B to E in OSA patients was the higher. In the R/R-OH/OA stage, the curves of the two groups almost overlapped.

Table 2  
Microstate parameters of healthy controls in each sleep stage

		Gev		MeanDur		TimeCov		SegDensity	
		Average	S.D.	Average	S.D.	Average	S.D.	Average	S.D.
N1	A	23.7	2.3	100.0	0.0	24.0	2.0	24.0	2.0
	B	23.5	2.6	100.0	0.0	24.0	2.0	24.0	2.0
	C	25.2	3.7	110.0	30.0	26.0	4.9	24.0	2.0
	D	25.7	4.2	100.0	0.0	26.0	4.9	26.0	4.9
N2	A	24.8	0.4	100.0	0.0	25.4	1.1	25.3	1.1
	B	24.8	0.3	110.0	30.0	25.4	1.1	23.9	3.2
	C	25.1	0.5	110.0	30.0	25.4	1.1	23.9	3.2
	D	23.7	3.2	100.0	0.0	23.9	3.2	23.9	3.2
N3	A	24.8	0.4	100.0	0.0	25.0	0.0	25.0	0.0
	B	24.9	0.1	100.0	0.0	25.0	0.0	25.0	0.0
	C	24.8	0.1	100.0	0.0	25.0	0.0	25.0	0.0
	D	25.0	0.0	100.0	0.0	25.0	0.0	25.0	0.0
R	A	25.9	3.0	111.1	31.4	26.7	4.7	24.4	1.6
	B	24.2	1.9	100.0	0.0	24.4	1.2	24.4	1.6
	C	24.1	2.0	100.0	0.0	24.4	1.2	24.4	1.6
	D	24.4	1.6	100.0	0.0	24.4	1.2	24.4	1.6

Table 3

Microstate parameters of OSA patients in each sleep stage. OSA patients have an additional microstate E in N1-OH/OA and N3-OH/OA stages. Compared with microstates A, B, C and D, microstate E has lower GEV, MeanDur, TimeCov, and SegDensity, only 2.3 ~ 2.5%, 22.2 ~ 22.3 ms and 2.3 ~ 2.9%.

		Gev		MeanDur		TimeCov		SegDensity	
		Average	S.D.	Average	S.D.	Average	S.D.	Average	S.D.
N1-OH/OA	A	23.2	3.0	100.0	0.0	23.9	2.9	23.9	2.9
	B	22.8	4.0	100.0	0.0	23.5	3.8	23.5	3.8
	C	24.0	3.3	118.5*	38.9	25.1	3.6	22.5	4.6
	D	24.1	5.1	112.6*	41.2	24.5	5.7	22.5	4.6
	<b>E</b>	<b>2.5</b>	<b>4.8</b>	<b>22.2</b>	<b>41.2</b>	<b>2.9</b>	<b>5.4</b>	<b>2.9</b>	<b>5.3</b>
N2-OH/OA	A	24.1	2.3	103.6	18.6	24.7	2.7	24.1	2.6
	B	25.0	3.6	105.1	19.8	25.9	4.6	24.7	1.9
	C	24.0	2.1	100.0	0.0	24.7	1.9	24.7	1.9
	D	24.6	2.5	103.6	18.6	24.7	2.7	24.1	2.6
N3-OH/OA	A	24.9	0.3	100.0	0.0	25.3	1.0	25.3	1.0
	B	23.6	3.0	100.0	0.0	24.0	3.1	24.0	3.1
	C	24.0	3.1	100.0	0.0	24.0	3.1	24.0	3.1
	D	26.0	3.6	118.1*	47.4	26.6	5.1	24.0	3.1
	<b>E</b>	<b>2.3</b>	<b>4.6</b>	<b>22.3</b>	<b>42.3</b>	<b>2.3</b>	<b>5.8</b>	<b>2.7</b>	<b>5.5</b>
R-OH/OA	A	26.7*	2.8	100.0	0.0	27.8	7.9	27.8	7.9
	B	22.8	4.7	100.0	0.0	22.2	7.9	22.2	7.9
	C	26.0	1.0	100.0	0.0	25.0	0.0	25.0	0.0
	D	25.0	1.0	100.0	0.0	25.0	0.0	25.0	0.0

Stars represent significant difference in five frequency bands between the two groups (Bonferroni corrected: P\* < 0.05, P\*\* < 0.05).

## Power spectrum, sample entropy and DFA of OSA patients

Through independent sample *t*-test, there is significant difference between power spectrum of two groups in beta band in N1 phase ( $P < 0.026$ ), in sigma band in N2 phase ( $P < 0.02$ ), in delta, theta and alpha band in N3 phase ( $P < 0.021$ ;  $P < 0.047$ ;  $P < 0.007$ ), and in beta band in R phase ( $P < 0.021$ ). And there are significant differences between sample entropy ( $p < 0.015$ ;  $p < 0.045$ ;  $p < 0.035$ ;  $p < 0.036$ ) and FDA ( $p < 0.005$ ;  $p < 0.001$ ;  $p < 0.005$ ;  $p < 0.005$ ) of OSA patients and healthy controls in four sleep stages.

The power spectrum of two groups in the delta, theta, alpha, sigma and beta band in four stages is shown in Fig. 4. It can be seen that the delta power spectrum of the two groups exceeds 50% in the range of 0.5 ~ 32 Hz, but significant difference only in N3-OH/OA phase ( $P < 0.021$ ). Stars indicate p-values of the independent sample t-test below the threshold for significance (Bonferroni corrected,  $*p < 0.05$ ,  $**p < 0.005$ ) in five bands of two groups in Fig. 4.

The sample entropy of two groups in four stages is shown in Fig. 5 (a). In the NREM stage, the sample entropy of two groups from N1 to N2 to N3 decreases continuously, but increases in R phase. And the sample entropy of OSA patients is lower than that of healthy controls (OSA vs. Control:  $1.2 \pm 0.01$  vs.  $1.4 \pm 0.02$  (N1);  $1.03 \pm 0.02$  vs.  $1.12 \pm 0.01$  (N2);  $0.72 \pm 0.02$  vs.  $0.81 \pm 0.01$  (N3);  $0.91 \pm 0.01$  vs.  $1.04 \pm 0.01$  (R)).

The scale index  $\alpha$  of two groups in four stages is shown in Fig. 5(b), and its scale index is  $0.5 < \alpha < 1.0$ , indicating that there is a long-range power-law correlation (with self-similarity of fractal dimension) in segmented time series. The scale index  $\alpha$  of OSA patients is higher than healthy controls in four sleep stages (OSA vs. control:  $0.90 \pm 0.02$  vs.  $0.73 \pm 0.02$  (N1);  $0.81 \pm 0.01$  vs.  $0.74 \pm 0.02$  (N2);  $0.90 \pm 0.01$  vs.  $0.72 \pm 0.02$  (N3);  $0.86 \pm 0.01$  vs.  $0.80 \pm 0.02$  (R)), and the scale index  $\alpha$  of OSA patients in N1-OH/OA and N3-OH/OA stages is higher than that in N2-OH/OA and R-OH/OA stages.

Figure 5 The sample entropy and scale index  $\alpha$  of two groups in four stages. In the NREM stage, the sample entropy of two groups from N1 to N2 to N3 decreases continuously, but increases in R phase. The sample entropy of OSA patients is lower than that of healthy controls. The scale index  $\alpha$  of OSA patients is higher than healthy controls in four sleep stages, and the scale index  $\alpha$  of OSA patients in N1-OH/OA and N3-OH/OA stages is higher than that in N2-OH/OA and R-OH/OA stages. Stars represent significant difference of two groups (Bonferroni corrected:  $P^* < 0.05$ ,  $P^{**} < 0.05$ ).

## Correlation between microstate parameters and power spectrum, sample entropy and DFA of OSA patients

Using *Pearson's* correlation analysis, the correlation between microstate parameters and power spectrum in alpha band in OSA patients is shown in Table 4. It can be seen that only in N1-OH/OA stage, microstate E is related to alpha power spectrum, and MeanDur of microstate E are negatively correlated ( $r = -0.430$ ,  $p = 0.028$ ). In N1-OH/OA stage, microstate E is also related to delta and theta power spectrum, shown in Appendix A and B. All microstate parameters in OSA patients are not related to sigma and beta power spectrum.

The microstate parameters in OSA patients are not correlated with sample entropy in four sleep stages, and their  $p$  values are shown in Table 5.

The correlation between microstate parameters and DFA in OSA patients is shown in Table 6. Only in N1-OH/OA stage, microstate C, D and E are related to DFA, SegDensity of microstate C and D are negatively correlated ( $r = -0.425$ ,  $p = 0.021$ ;  $r = -0.425$ ,  $p = 0.021$ ), and GEV, MeanDur, TimeCov and SegDensity of microstate E are all positively correlated ( $r = 0.394$ ,  $p = 0.046$ ;  $r = 0.396$ ,  $p = 0.045$ ;  $r = 0.416$ ,  $p = 0.045$ ;  $r = 0.416$ ,  $p = 0.045$ ).

Table 4

The correlation between microstate parameters and alpha power spectrum in OSA patients. Only in N1-OH/OA stage, MeanDur of microstate E is related to alpha power spectrum.

		Gev		MeanDur		TimeCov		SegDensity	
		Correlation coefficient	p-Value						
N1-OH/OA	A	-0.337	0.092	-0.359	0.072	-0.332	0.097	-0.332	0.097
	B	0.096	0.64	.a	.a	0.021	0.919	0.021	0.919
	C	0.165	0.421	.a	.a	0.113	0.583	0.113	0.583
	D	0.37	0.063	0.054	0.792	0.328	0.101	0.38	0.056
	E	<b>-0.042</b>	<b>0.840</b>	<b>-0.430*</b>	<b>0.028</b>	<b>-0.164</b>	<b>0.424</b>	<b>0.38</b>	<b>0.056</b>
N2-OH/OA	A	0.023	0.914	-0.066	0.753	0.009	0.965	0.089	0.672
	B	0.005	0.982	-0.066	0.753	0.009	0.965	0.089	0.672
	C	0.032	0.879	0.024	0.91	-0.007	0.975	-0.010	0.961
	D	-0.02	0.926	.a	.a	-0.010	0.961	-0.010	0.961
N3-OH/OA	A	-0.417	0.177	0.202	0.529	-0.143	0.658	-0.308	0.330
	B	-0.400	0.198	-0.394	0.205	-0.353	0.260	0.426	0.167
	C	0.160	0.619	.a	.a	0.143	0.658	0.143	0.658
	D	0.141	0.662	.a	.a	0.143	0.658	0.143	0.658
	E	0.202	0.529	0.202	0.529	0.202	0.529	0.202	0.529
R-OH/OA	A	0.023	0.914	-0.066	0.753	0.009	0.965	0.089	0.672
	B	-0.058	0.781	.a	.a	-0.121	0.565	-0.160	0.436
	C	0.154	0.463	.a	.a	0.143	0.496	0.143	0.496
	D	0.141	0.662	.a	.a	0.143	0.658	0.143	0.658
<b>* There was significant correlation at 0.05 level (bilateral).</b>									

.a Cannot be evaluated because at least one variable is constant.

Table 5

The correlation between microstate parameters and sample entropy in OSA patients. The microstate parameters are not correlated with sample entropy in four sleep stages.

		Gev		MeanDur		TimeCov		SegDensity	
		Correlation coefficient	p-Value						
N1-OH/OA	A	0.021	0.917	-0.009	0.965	-0.003	0.987	-0.003	0.987
	B	0.099	0.631	.a	.a	0.071	0.729	0.071	0.729
	C	0.105	0.611	.a	.a	0.102	0.619	0.102	0.619
	D	0.031	0.879	0.061	0.937	0.020	0.921	0.023	0.913
	E	-0.118	0.566	-0.099	0.63	-0.19	0.352	0.023	0.913
N2-OH/OA	A	0.125	0.551	0.093	0.659	0.131	0.533	0.027	0.899
	B	0.092	0.660	0.093	0.659	0.131	0.533	0.027	0.899
	C	-0.132	0.53	-0.049	0.818	-0.111	0.598	-0.105	0.616
	D	-0.131	0.533	.a	.a	-0.105	0.616	-0.105	0.616
N3-OH/OA	A	-0.218	0.496	0.182	0.572	-0.067	0.837	-0.252	0.430
	B	-0.273	0.391	-0.272	0.393	-0.235	0.463	0.307	0.332
	C	0.097	0.764	.a	.a	0.067	0.837	0.067	0.837
	D	0.063	0.846	.a	.a	0.067	0.837	0.067	0.837
	E	0.182	0.572	0.182	0.572	0.182	0.572	0.182	0.572
R-OH/OA	A	-0.132	0.53	.a	.a	0.067	0.837	0.067	0.837
	B	0.097	0.764	.a	.a	-0.121	0.565	-0.160	0.436
	C	0.154	0.463	.a	.a	0.143	0.496	0.143	0.496
	D	-0.131	0.533	.a	.a	0.061	0.859	0.061	0.859
.a Cannot be evaluated because at least one variable is constant.									

Table 6

The correlation between microstate parameters and FDA in OSA patients. Only in N1-OH/OA stage, microstate C, D and E are related to DFA.

		Gev		MeanDur		TimeCov		SegDensity	
		Correlation coefficient	p-Value						
N1-OH/OA	A	-0.205	0.315	.a	.a	-0.213	0.297	-0.213	0.297
	B	-0.160	0.436	.a	.a	-0.081	0.693	-0.081	0.693
	C	-0.366	0.066	0.24	0.237	-0.295	0.143	<b>-0.452*</b>	<b>0.021</b>
	D	-0.066	0.749	0.332	0.098	-0.038	0.853	<b>-0.452*</b>	<b>0.021</b>
	E	<b>0.394*</b>	<b>0.046</b>	<b>0.396*</b>	<b>0.045</b>	<b>0.416*</b>	<b>0.035</b>	<b>0.416*</b>	<b>0.035</b>
N2-OH/OA	A	0.163	0.437	0.081	0.701	0.143	0.496	0.054	0.799
	B	-0.121	0.565	-0.113	0.591	-0.145	0.49	-0.058	0.781
	C	0.002	0.991	.a	.a	-0.058	0.781	-0.058	0.781
	D	0.154	0.463	0.081	0.701	0.143	0.496	0.054	0.799
N3-OH/OA	A	-0.717	0.614	.a	.a	-0.061	0.859	-0.061	0.859
	B	0.116	0.735	.a	.a	0.061	0.859	0.061	0.859
	C	0.061	0.859	.a	.a	0.061	0.859	0.061	0.859
	D	-0.042	0.903	-0.061	0.859	-0.061	0.859	0.061	0.859
	E	0.006	0.748	0.332	0.087	0.143	0.496	0.054	0.799
R-OH/OA	A	0.163	0.437	.a	.a	0.154	0.463	0.154	0.463
	B	-0.058	0.781	.a	.a	-0.121	0.565	-0.160	0.436
	C	0.154	0.463	.a	.a	0.143	0.496	0.143	0.496
	D	0.116	0.735	.a	.a	0.061	0.859	0.061	0.859

\* There was significant correlation at 0.05 level (bilateral).

.a Cannot be evaluated because at least one variable is constant.

## Discussion

We compared the microstate, power spectrum, sample entropy and DFA in four sleep stages between OSA patients and healthy controls. We found that OSA patients had an additional fifth microstate E in N1-OH/OA and N3-OH/OA stages, and microstate E was related to delta, theta and alpha power spectrum and DFA in N1-OH/OA stage.

As shown in Table 1, OSA may occur in any stage of sleep cycle, but the number of OH/OA occurrences in N1 and N2 stages is more than that in N3 stage. The pathogenesis of OSA is upper airway stenosis and obstruction<sup>3</sup>. Breathing can stop temporarily for ten seconds or even several minutes, and it can happen hundreds of times a night, leading to hypoxia, which makes the patient wake up suddenly and is difficult to enter deep sleep. Therefore, because the frequent occurrence of OH/OA causes the patient to repeatedly switch between light sleep stage (N1, N2) and wakefulness, it is difficult to enter the deep sleep stage (N3).

Microstate reflects the instantaneous state of the brain, and can identify discontinuous and nonlinear changes of global functional brain state under very high temporal resolution<sup>12, 15</sup>. It has been found that four canonical microstates A, B, C and D are related to the activities of the posterior cingulate cortex<sup>21</sup>. Combined fMRI-EEG imaging studies have shown that the neural components that generate microstates overlap with the resting-state network independently recognized by fMRI<sup>22, 23, 24</sup>. Brodbeck et al. investigated wakefulness and NREM sleep of healthy subjects, and found that microstate C was dominant in W, N1 and N3 stages, while microstate B was dominant in N2 stage. With the increase of sleep depth, the parameter GEV of microstate D gradually decreased<sup>16</sup>. Kuhn et al. investigated early NREM sleep of narcoleptic patients, and found that microstate C and D were dominant in N1 stage, microstate D was still dominant in N2 and N3 stages, and an extra microstate E appeared in N3 stage<sup>17</sup>. The authors thought that the occurrence of extra microstate E in N3 stage indicated that the corresponding neural network activity was unstable and led to fragmented sleep structure<sup>17</sup>.

Through the microstate analysis in four sleep stages in OSA patients and healthy controls, we found that OSA patients had an additional fifth microstate E in N1-OH/OA and N3-OH/OA stages, and the duration of microstate C and D was longer. The possible reason is that due to the frequent occurrence of OH/OA, the activity of the neural network that generates microstates C and D is unstable or has changed in N1-OH/OA and N3-OH/OA stages, which in turn splits the microstate E. The GEV of microstate E is low, only 2.3 ~ 2.5%, and MeanDur is also short, 22.2 ~ 22.3 ms. After fitting the microstates A, B, C, D and E back to the original EEG signals, we found that the microstate E only existed on a few patients' EEG signals. This shows that the probability of occurrence of microstate E is lower and the variability is relatively large among different subjects. In addition, we found that OSA patients had an additional microstate E in N1-OA/OH and N3-OA/OH stages, but microstate E in N1-OA/OH stage was related to delta, theta and alpha power spectrum and DFA, not related in N3-OA/OH stage. The possible reason is that the OSA patients we screened have large differences among individuals or because our sample size is too small, resulting in insufficient statistical power. In future studies, increasing the sample size of OSA patients may be able to further verify this result.

There were previous studies on the difference of wakefulness EEG power between OSA patients and healthy controls<sup>8, 9</sup>, but there were few studies on the changes of sleep EEG power in OSA patients. Delta rhythm (0.5 ~ 4.5 Hz) mainly occurs in deep sleep or coma, during which human is difficult to wake up, and human's cortical activities lose sensory input, that is, the separation of cortical activity and thalamic activity. We found that the delta band power of OSA patients in N3-OA/OH was higher than healthy controls ( $P < 0.021$ ).

Grenèche and D'Rozario also found delta band power increased in OSA patients in wakefulness state<sup>8, 9</sup>. These studies show that delta power increases in OSA patients both in wakefulness and sleeping states. Monegro et al. investigated delta power in OSA patients before and/or after therapy with Continuous Positive

Airway Pressure (CPAP), and found that there was an overall decrease in delta power in patients with a higher Respiratory Disturbance Index (RDI) after CPAP<sup>25</sup>. These studies show that hypoxia is related to the changes of brain delta power. It is known that there is a coupling relationship between neuroelectrophysiology and hemodynamics, and the cerebral blood flow and intracranial pressure increase in OSA patients due to a certain degree of hypoxia, which may cause delta power increase. The cerebral hypoxia is relieved after CPAP, and the relief effect is more obvious for patients with higher RDI. In addition to hypoxia, EEG changes are also related to age, including increased slow wave and lower alpha power<sup>26</sup>, so the slower EEG in OSA patients may not only be caused by sleep disorders, but may also be related to age<sup>9</sup>. In our study, the age information of 10 healthy subjects is missing in the ISRUC-Sleep data set, so further analysis of age factors is not possible.

Beta rhythm (the frequency range of beta rhythm in some literatures is 13 ~ 30 Hz, which is divided into sigma (12 ~ 15 Hz) and beta (15 ~ 32 Hz) in this study) mainly appears in the active state of brain such as active thinking. In the late stage of light sleep (N1), low-amplitude beta waves may appear. In our study, the beta power of OSA patients was lower than healthy controls in N1-OA/OH stage ( $P < 0.026$ ), and sigma power of OSA patients was lower than healthy controls in N2-OA/OH stage. Grenèche et al. found that the beta power of wakefulness EEG in OSA patients was higher than healthy subjects, but in their study, OSA patients were during resting state and did not move or imagine movement<sup>8</sup>. D'Rozario et al. did not report beta band power<sup>9</sup>. Previous studies show that beta rhythms decrease (i.e., event-related desynchronization (ERD)) during movement imagery, movement preparation and movement execution<sup>27</sup>. We infer that OSA patients during the N1 and N2 stages with frequent apneas, by changing their body posture to relieve the discomfort caused by apneas, and thus show a decrease in beta power.

Through *Pearson* correlation analysis, microstate E was related to delta, theta and alpha power in N1-OH/OA stage, and the sigma and beta power were independent of all microstates in all sleep stages. Previous studies revealed no conclusive results concerning the association of the four EEG microstate classes with specific power spectral distributions<sup>22, 23</sup>. However, Milz et al. investigated head-surface localization- or source-dependent power effects on the occurrence of the EEG microstate classes, and found that the EEG microstate topography was predominantly determined by intracortical sources in the alpha band<sup>28</sup>. Croce et al. investigated EEG microstates associated with intra- and inter-subject alpha variability, and observed an increase in the metrics of microstate B, with the level of intra-subject amplitude alpha oscillations, together with lower coverage of microstate D and a higher frequency of microstate C<sup>29</sup>. Although their study found the relationship between alpha power and microstate metrics, the authors also pointed out that there was no specificity for alpha power. The modulation effect on microstate metrics is not unique to the alpha band. It may be caused by fluctuations in other frequency bands<sup>29</sup>. Therefore, we can infer that when apnea occurred in N1 and N3 stages, the intensity and spatial distribution of alpha activity in the cortex changed, which induced microstate E. Or because of the mediation by alpha band and the dynamic interaction with other bands (such as delta, theta bands), the original scalp potential distribution is changed, and an additional microstate E is generated.

Sample entropy is an improved method for measuring the complexity of time series, and it has applications in evaluating the complexity of physiological time series and diagnosing pathological state<sup>18, 30, 31</sup>. Zhou et al.

found that the sample entropy of sleep apnea syndrome patients was lower than that of healthy controls in each sleep stage<sup>7</sup>. We found that the sample entropy of OSA patients was lower than healthy controls in four sleep stages ( $P < 0.05$ ). According to the dynamic theory of entropy, the greater the entropy is, the higher the complexity of the sequence. Low entropy indicates that the data is highly predictable and regular, while high entropy indicates that the data is chaotic and unpredictable. Meaningful and complex data have intermediate entropy. When human is awake, the brain receives information from the outside world and is still carrying out complex thinking activities, and the neurons are active, therefore EEG signals present complex randomness. With the deepening of sleep, the activity of neurons in the brain gradually decreases and the synchronization orderly increases. The EEG signals show more regular characteristics of self-regulation, of which the complexity decreases. In REM stage, along with physiological activities such as dream and eye rotation, the brain nerve activity increases and the EEG complexity increases<sup>7</sup>. Therefore, the change of sample entropy reflects the physiological mechanism of sleep, as shown in Fig. 5 (a). The sample entropy of OSA patients is lower than healthy controls. The possible reason is that brain hypoxia or other pathological conditions caused by OSA have a significant impact on brain nerve activity, resulting in a significant decrease in the activity and complexity of brain cells<sup>7</sup>.

Through *Pearson* correlation analysis, our results showed that the microstate parameters GEV, MeanDur, TimeCov and SegDensity in OSA patients were not correlated with the sample entropy in four sleep stages, and their  $p$  values are shown in Table 5. Murphy et al. employed sample entropy to calculate the complexity of the microstate sequence over the entire template length in subjects with psychotic disorders<sup>18</sup>. They thought that the transition of microstate was independent of the duration of microstate, so they deleted the information of microstate duration. In this way, the microstate sequence was compressed. Their results showed that there was no correlation between sequence length and entropy in psychiatric patients and healthy controls, and there was no statistically significant correlation between entropy and microstate duration at any pattern length of sample entropy<sup>18</sup>. While our study showed that sample entropy was not only independent of the duration of microstates, but also irrelevant to GEV, TimeCov and SegDensity of microstates. The difference was that Murphy et al. calculated the sample entropy on the compressed microstate sequence with template length  $m = 3 \sim 10$ , while we calculated the sample entropy on the preprocessed EEG signal with template length  $m = 2$ . Although these studies differ in details, they all show that the microstate sequence has nothing to do with the complexity of EEG signals.

EEG signal has a long-term correlation of dynamic oscillation characteristics<sup>32,33</sup>. Detrended fluctuation analysis (DFA) quantifies the time-domain fluctuation of time series by power-law method, and describes the scaling behavior or long-range correlation of time series with scale index, which is suitable for studying the correlation of long-range power-law functions of various unstable time series. Our study showed that the scale index of OSA patients and healthy controls was  $0.5 < \alpha < 1.0$ , which indicated that there was a long-range power-law continuous correlation of EEG signal (with self-similarity of fractal dimension). The scale index  $\alpha$  of OSA patients was higher than healthy controls in four sleep stages, and the scale index  $\alpha$  of OSA patients in N1-OH/OA and N3-OH/OA was higher than that of N2-OH/OA and R-OH/OA, as shown in Fig. 5 (b). D’Rozario et al. found that the DFA of the OSA patients was higher than healthy controls with eyes opening and closing, and the DFA of the two groups with eyes opening was higher than that with eyes closing<sup>9</sup>. Our study results were basically consistent with theirs. From the fractal dynamics, when the scale index  $\alpha$  is

between 0.5 and 1, the larger the value is, the stronger the self-similarity regularity of the signal is, which means that the information entropy is lower (when the value is 1, it is  $1/f$  noise); conversely, the smaller the value is, the stronger the randomness of the signal is, which means that the information entropy is higher (when the value is 0.5, it appears as white noise)<sup>34</sup>. This indicates that the EEG signals of OSA patients have stronger self-similar regularity than healthy controls, especially in N1-OH/OA and N3-OH/OA stages. The oscillation mode is smoother, which may be caused by abnormal changes of brain activity conversion in OSA patients in these two stages. The reasons for the differences in the long-range power function correlations of EEG signals in different populations and in different physiological and pathological states have not been fully clarified. Some studies have speculated that this was related to the special mechanism of neural oscillation. The differences in scale behavior or long-range correlation reflect that neuronal oscillations may be affected by special mechanisms related to their origin<sup>33</sup>.

Through *Pearson* correlation analysis, our results showed that microstate C, D and E were correlated with DFA in OSA patients in N1-OH/OA stage, and GEV, MeanDur, TimeCov and SegDensity of microstate E were positively correlated with DFA. Previous studies have shown that the microstate of healthy subjects exhibit scale-free and self-similar dynamic characteristics<sup>35</sup>. Murphy et al. carried out fractal analysis on the microstate of psychiatric patients, and found that the microstate sequence has a long-term time-dependent<sup>18</sup>. This shows that the microstate is the same as the scale index  $\alpha$ , which reflects the self-similarity of EEG signals.

At present, there is no simple and effective EEG biomarker that can reflect the negative impact of OSA on the brain, although D'Rozario et al. have shown that the DFA scale index has the potential as an EEG biomarker of neurobehavioral damage<sup>9</sup>. However, their study only compared DFA and power spectrum, and lacked comparative analysis with other EEG biomarkers (such as sample entropy, microstate, etc.). In addition, they only considered the single scene of simulated driving, and lacked the research on sleep EEG and its prognostic value. In our study, the sleep EEG of OSA patients was analyzed by the microstate method and the correlation analysis with power spectrum, sample entropy and DFA was carried out, and the additional microstate E was found, which was related to the power spectrum of delta, theta and alpha bands and DFA. This shows that the microstate also has the potential as a biomarker of OSA EEG. Zappasodi et al. investigated prognostic value of EEG microstates in acute stroke, and found that a preserved microstate B in acute phase correlated with a better effective recovery<sup>36</sup>. Therefore, whether there is a correlation between microstate and OSA score and whether it has prognostic value for OSA patients is our next research work.

Finally, fewer EEG channels were employed for the microstate analysis in our study, only 6 channels<sup>37</sup>, but previous studies have demonstrated that canonical microstate topographic maps are not limited by low spatial sampling<sup>18, 38</sup>. In the past 20 years, researchers have conducted many studies using microstate analysis, exploring the topography, duration, frequency and transition probability of microstates. But the interpretation of these studies is complicated by the small sample size and the differences in analytical techniques. Even in the study of canonical four microstates, there are major differences regarding the microstate topographic maps, especially for microstates C and D<sup>39</sup>. Michel et al. considered that the number of topographic map should not be a fixed value (for example, 4), but the optimal number of topographic map should be estimated according to the specific situation of data sets<sup>39</sup>. Therefore, the results of microstate

analysis, especially the number of microstates generated, should be treated with caution. The limitation of this study is that the sample size is limited. OSA patients with other complications and taking drugs were excluded in our study. Whether these two types of patients affect the conclusion of this paper needs further study.

## Methods

### Data sources

The polysomnography (PSG) recordings come from an open-access sleep dataset, ISRUC-Sleep (<http://sleeptight.isr.uc.pt/> ISRUC\_Sleep). The data were obtained from healthy subjects, subjects with sleep disorders, and subjects under the effect of sleep medication (i.e., Subgroup\_I, Subgroup\_II, Subgroup\_III), from all-night PSG records, each with duration around 8 h, which were acquired by the Sleep Medicine Centre of the Hospital of Coimbra University (CHUC)<sup>37</sup>. All EEG, EOG, and EMG (chin) recordings were performed with a sampling rate of 200 Hz and stored into computer files using the standard EDF data format. The PSG recordings were composed by signals from 19 channels, of which EEG signal had 6 channels (F3, C3, O1, F4, C4 and O2). All recordings were segmented into epochs of 30 s and visually labeled by two experts according to the guidelines of AASM<sup>40</sup>, with the stages: awake (W), NREM (including N1, N2 and N3) and REM (abbreviated as R) sleep. Our dataset came from 30 OSA patients (excluding patients with other complications and taking medications) from Subgroup\_I and 10 healthy subjects from Subgroup\_III.

### EEG data pre-processing

EEG signals were pre-processed with the EEGLAB toolbox for MATLAB, which were re-referenced to the common average reference, high-pass filtered with a 0.1 Hz zero-phase FIR filter, low-pass filtered with a 45 Hz zero-phase FIR filter, and down-sampled to 100 Hz. EEG signals were inspected for artifacts with a procedure based on Independent Components (ICs) using ADJUST plug-in<sup>41</sup>. IC scalp maps and frequency spectra were inspected, and ICs that displayed features indicative of artifacts were removed<sup>42</sup>.

For OSA patients, EEG epochs were extracted for each patient when labeled OH (Obstructive Hypopnea) or OA (Obstructive Apnea). For healthy controls, epochs were extracted from each healthy subject in each sleep stage (W, N1, N2, N3 and R). An epoch lasted for 30 s, and 10 epochs were extracted in each sleep stage.

### Microstate analysis

Microstates reflect the instantaneous state of the brain, and can identify global functional brain states at very high temporal resolution. EEG microstates were extracted from each subject with the CARTOOL software<sup>19</sup> by using a polarity-insensitive K-means algorithm in each epoch. The optimal number of microstates was determined by means of a combination of cross-validation and the Krzanovski-Lai criteria<sup>13</sup>. The same number of microstates was retained for each subject. The microstate maps of each subject were then submitted to a second cluster analysis in order to identify the dominant maps across the subjects<sup>43</sup>. Statistical smoothing was applied to remove temporally isolated topographic maps with low explanatory power. Clusters that correlated above 90% were merged, and segments shorter than 10 ms were rejected. The reference maps were selected as those that highly spatially correlated with the other maps in the same

cluster. The microstate maps of each subject were matched with the reference maps showing the higher spatial correlation.

## Power spectral analysis

Previous research has shown that power spectrum analysis of wakefulness EEG is helpful to detect human's alertness<sup>44, 45, 46</sup>. Greneche et al. have compared the power spectrum of wakefulness EEG between OSA patients and healthy controls<sup>8</sup>, but we focused on the power spectrum of sleep EEG between OSA patients and healthy controls. After artefactual epochs were rejected, power spectrum was obtained using a standard fast Fourier transform (FFT) with a rectangular weighting window<sup>47</sup>, for each non-overlapping 5 s epoch of EEG, i.e., 500 data points<sup>9, 10</sup>. Absolute power spectra was calculated in the delta, theta, alpha, sigma and beta bands in each frequency ranges of 0.5 ~ 4.5, 4.5 ~ 8, 8 ~ 12, 12 ~ 15 and 15 ~ 32 Hz. Power spectrum in each sleep-staged 30 s epoch was calculated by averaging data from 6 5 s epochs. Absolute power spectrum was used to calculate to power density. For example, delta power density is equal to absolute power in the 0.5 ~ 4.5 Hz frequency range divided by the sum of absolute powers in 0.5 ~ 32 Hz frequency ranges.

## Sample entropy analysis

Sample entropy is a method to measure the complexity of time series, which has been successfully applied in the analysis of physiological signals, such as heart rate, blood pressure, EEG, etc.. Its calculation results are related to the selection of parameters  $m$ ,  $r$  and  $n$ <sup>48</sup>. (1) The embedding dimension  $m$  represents the length of the sequence. Generally,  $m$  is set to 1 or 2, because when  $m > 2$ , the amount of data  $n$  is required to be more than several thousand points<sup>48</sup>. (2) The physical meaning of threshold  $r$  is the radius of super ball with dimension  $m$ , which is a parameter to measure the similarity of time series, which can be set according to the needs of specific problems. Pincus believed that when  $r$  was set to  $(0.1 \sim 0.25) \times SD$  ( $SD$  was the standard deviation), and the effective statistical characteristics could be obtained<sup>48</sup>. (3) The input data point  $n$  is set to 100 ~ 5000 in order to get effective statistical characteristics and small pseudo error for the given data. Therefore, in our study, we took  $m = 2$ ,  $r = 0.2SD$  and  $n = 1000$ .

## Detrended fluctuation analysis

Detrended fluctuation analysis (DFA) is widely used to analyze the long-range correlation of various unsteady signals, such as ECG, EEG, DNA sequence, weather signal, turbulence velocity and temperature field. DFA is an improved root mean square analysis method, which has two advantages over the commonly used fractal analysis methods: (1) it can detect the self-similarity of time series signal that seems to be unstable but is inherently self-similarity; (2) it can avoid the obvious self-similarity trend caused by external factors<sup>49</sup>.

The function relationship curve of the DFA wave function  $F(s)$  and the interval length  $s$  is drawn in double logarithmic coordinates, then the slope of the curve by linear fitting is calculated, which is the scale index  $\alpha$ . The scale index  $\alpha$  provides a quantitative index for the correlation of the long-range power function. If  $\alpha < 0.5$ , it means that the segmented time series are independent of each other; if  $0.5 < \alpha < 1.0$ , it means that the segmented time series have continuous correlation in the form of long-range power rate (with self-similarity of fractal dimension); if  $\alpha = 1$ , it indicates that the segmented time series fluctuate in the form of  $1/f$  noise; if  $1.0 < \alpha < 1.5$ , it means that the segmented time series do not have long-range correlation; if  $\alpha = 1.5$ , it indicates

that the segmented time series are Brownian noise, that is, they are random independent. In our study, we took the data length  $n = 1000$ , and divided the sequence into 80 non-overlapping segments, and the corresponding data lengths were 10, 15, 20, ..., 405<sup>34</sup>

## Statistical analysis

In order to compare the difference of EEG signals between OSA patients and healthy controls, independent sample  $t$  test was conducted on the significance level of microstate parameters, power, sample entropy and FDA between the two groups, and Bonferroni corrected. In addition, *Pearson* correlation test was used to verify the correlation between microstate parameters and power, sample entropy and FDA. All statistical analyses were performed using IBM SPSS statistics, version 21 (IBM Corp., Armonk, NY, USA), and  $P < 0.05$  was considered statistically significant.

## Declarations

### Conflict of Interest Statement

None of the authors have potential conflicts of interest to be disclosed.

### Acknowledgments

This study was funded by Grant Nos. 82060329, 11265007 from National Natural Science Foundation of China (NSFC), No. 2020J0052 from Scientific Research Fund Project of Yunnan Education Department of China.

## References

1. Heinzer R, Vat S, Marques-Vidal P, Marti-Soler H, Andries D, Tobback N, et al.. Prevalence of sleep-disordered breathing in the general population: the HypnoLaus study. *Lancet Respir Med* 2015; 3(4):310-318.
2. Young T, Peppard P, Palta M, Hla K, Finn L, Morgan B, et al.. Population-based study of sleep-disordered breathing as a risk factor for hypertension. *Arch Intern Med* 1997; 157(15): 1746-1752.
3. Eckert DJ, Malhotra A. Pathophysiology of adult obstructive sleep apnea. *Proc Am Thorac Soc* 2008;5(2):144-153.
4. George CF. Sleep apnea, alertness, and motor vehicle crashes. *Am J Respir Crit Care Med* 2007;176: 954-956.
5. Aksahin M, Aydin S, Firat H, Erogul O. Artificial apnea classification with quantitative sleep EEG synchronization. *J Med Syst* 2012; 36 (1): 139-144.
6. Liu D, Pang Z, Lloyd SR. Aneural network method for detection of obstructive sleep apnea and narcolepsy based on pupil size and EEG. *IEEE Trans Neural Netw* 2008; 19(2): 308-18.
7. Zhou J, Wu XM. Electroencephalogram of sleep apnea syndrome based on sample entropy. *Chinese Journal of Medical Physics* 2016; (7):722-725.

8. Grenèche J, Krieger J, Erhardt C, Bonnefond A, Eschenlauer A, Muzet A, et al. EEG spectral power and sleepiness during 24 h of sustained wakefulness in patients with obstructive sleep apnea syndrome. *Clin Neurophysiol* 2008; 119: 418-428.
9. D’Rozario, Angela L, Kim JW , Wong K. A new EEG biomarker of neurobehavioural impairment and sleepiness in sleep apnea patients and controls during extended wakefulness. *Clin Neurophysiol* 2013; 124(8): 1605-1614.
10. Vakulin A , D’Rozario, Angela, Kim J W. Quantitative sleep EEG and polysomnographic predictors of driving simulator performance in obstructive sleep apnea. *Clin Neurophysiol* 2015; 127:1428-1435.
11. Jong Won Kim, Shin HB, Robinson PA. Quantitative study of the sleep onset period via detrended fluctuation analysis: Normal vs. narcoleptic subjects. *Clin Neurophysiol* 2009; 120: 1245-1251.
12. Lehmann D, Ozaki H, Pal I. EEG alpha map series: brain micro-states by space-oriented adaptive segmentation. *Electroencephalography and Clinical Neurophysiology* 1987; 67: 271–288.
13. Murray MM, Brunet D, Michel CM. Topographic ERP analyses: a step-by-step tutorial review. *Brain Topogr.* 2008; 20, 249–264.
14. Zappasodi F, Croce P, Giordani A, et al. Prognostic Value of EEG Microstates in Acute Stroke. *Brain Topography*, 2017, 30(5):1-13.
15. Khanna A, Pascual-Leone A, Michel C, Farzan F. Microstates in resting-state EEG: Current status and future directions. *Neuroscience & Biobehavioral Reviews* 2015; 49: 105-113.
16. Brodbeck V, Kuhn A, Wegner FV, Morzelewski A. EEG microstates of wakefulness and NREM sleep. *NeuroImage* 2012; 62(3):2129-39.
17. Kuhn A, Brodbeck V, Tagliazucchi E, Morzelewski A. Narcoleptic Patients Show Fragmented EEG-Microstructure During Early NREM Sleep. *Brain Topography* 2014; 28(4):619-635.
18. Murphy M, Stickgold R, Öngür D. Electroencephalogram Microstate Abnormalities in Early-Course Psychosis, *Biological Psychiatry: Cognitive Neuroscience and Neuroimaging* 2020; 5(1):35–44.
19. Brunet D, Murray MM, Michel CM. Spatiotemporal analysis of multichannel EEG: cartool. *Comput. Intell. Neurosci.* 2011; 813-870.
20. Pascual-Marqui RD, Michel CM, Lehmann D. Segmentation of brain electrical activity into microstates: model estimation and validation. *IEEE Trans. Biomed. Eng.* 1995; 42: 658–65.
21. Pascual-Marqui RD , Lehmann D , Faber P , Milz P, Kochi K, Yoshimura M, et al. The resting microstate networks (RMN): cortical distributions, dynamics, and frequency specific information flow. *Quantitative Biology*; 2014.
22. Britz J, Van De Ville D, Michel CM. BOLD correlates of EEG topography reveal rapid resting-state network dynamics. *Neuroimage* 2010; 52:1162–1170.
23. Musso F, Brinkmeyer J, Mobascher A, Warbrick T, Winterer G. Spontaneous brain activity and EEG microstates. A novel EEG/fMRI analysis approach to explore resting-state networks. *Neuroimage* 2010; 52:1149–1161.
24. Yuan H, Zotev V, Phillips R, Drevets WC, Bodurka J. Spatiotemporal dynamics of the brain at rest— Exploring EEG microstates as electrophysiological signatures of BOLD resting state networks. *Neuroimage* 2012; 60:2062–2072.

25. Monegro A F , Sahota P K , Bollu P C , et al. 0542 Delta power in Obstructive Sleep Apnea with predominant Respiratory Effort Related Arousals before and after therapy with Continuous Positive Airway Pressure. *Sleep*, 2019, 42(Supplement\_1):A216-A217.
26. Chiang AK, Rennie CJ, Robinson PA, van Albada SJ, Kerr CC. Age trends and sex differences of alpha rhythms including split alpha peaks. *Clin Neurophysiol* 2011;122:1505–
27. Pfurtscheller G and Lopes da Silva F H 1999 Event-related EEG/MEG synchronization and desynchronization: basic principles *Clin. Neurophysiol.* 110 1842–57
28. Milz P, Pascual-Marqui RD, Achermann P, Kochi K, Faber PL. The EEG microstate topography is predominantly determined by intracortical sources in the alpha band. *Neuroimage* 2017; 162:353–361.
29. Croce, P., Quercia, A., Costa, S. & Zappasodi, F. EEG microstates associated with intra- and inter-subject alpha variability. *Sci Rep* 10, 2469 (2020).
30. Takahashi T. Complexity of spontaneous brain activity in mental disorders. *Prog Neuropsychopharmacol Biol Psychiatry* 2013; 45:258–266.
31. Fernández A, Gómez C, Hornero R, López-Ibor JJ. Complexity and schizophrenia. *Prog Neuropsychopharmacol Biol Psychiatry* 2013; 45:267–276.
32. Watters P A, Martin F. A method for establishing long-range power law correlation from the electroencephalogram. *Biol Psychiatry* 2004; 66:79-89
33. Nikulin VV, Brismar T. Long-range temporal correlation in electroencephalographic oscillations: relation to topography, frequency band, age and gender. *Neuroscience* 2005; 130:549-558.
34. Wang CF, Zhang LX, Liu S, Sun CC, Wang YJ, Zhao X, et al. Feature Extraction and Recognition of Resting EEG in Poststroke Depression Subjects Based on Detrended Fluctuation Analysis. *Chinese Journal of Biomedical Engineering* 2013; 32(5): 520-525.
35. Ville DV, Britz J, Michel CM. EEG microstate sequences in healthy humans at rest reveal scale-free dynamics. *Proceedings of the National Academy of Sciences* 2010; 107(42):18179-18184.
36. Zappasodi F , Croce P , Giordani A , et al. Prognostic Value of EEG Microstates in Acute Stroke[J]. *Brain Topography*, 2017.
37. Khalighi S, Sousa T, Santos J, Nunes U. ISRUC-Sleep: A comprehensive public dataset for sleep researchers. *Computer Methods and Programs in Biomedicine* 2016; 124: 180-192.
38. Khanna A, Pascualleone A, Farzan F. Reliability of Resting-State Microstate Features in Electroencephalography. *PLoS ONE* 2014; 12: 1-12.
39. Michel CM, Koenig T. EEG microstates as a tool for studying the temporal dynamics of whole-brain neuronal networks: A review. *Neuroimage* 2018; 180(pt B):577–593.
40. Iber C, Ancoli-Israel S, Chesson A, Quan S. The AASM manual for the scoring of sleep and associated events: Rules terminology and technical specifications, 2007.
41. Brunner C, Delorme A, Makeig S. EEGLAB – An Open Source MATLAB Toolbox for Electrophysiological Research. *Biomedical Engineering* 2013; 58: 3234
42. Mognon A, Jovicich J, Bruzzone L, Buiatti M. [ADJUST: An automatic EEG artifact detector based on the joint use of spatial and temporal features.](#) *Psychophysiology* 2011; 2:229-240.

43. Minguillon J, Pirondini E, Coscia M, Leeb R. Modular organization of reaching and grasping movements investigated using EEG microstates. Engineering in Medicine & Biology Society. IEEE, 2014.
44. Higuchi S, Liu Y, Yuasa T, Maeda A, Motohashi Y. Diurnal variation in alpha power density and subjective sleepiness while performing repeated vigilance tasks. Clin Neurophysiol 2001; 112: 997-1000.
45. Sforza E, Grandin S, Jouny C, Rochat T, Ibanez V. Is waking electroencephalographic activity a predictor of daytime sleepiness in sleep-related breathing disorders? Eur Respir J 2002; 19: 645-652.
46. Wang CW, Guragain B, Verma A, Archer L. Spectral Analysis of EEG during Microsleep Events Annotated via Driver Monitoring System to Characterize Drowsiness. IEEE Transactions on Aerospace and Electronic Systems 2020; 56(2):1346-1356.
47. Press WH, Teukolsky SA, Vetterling WT, Flannery BP. Numerical Recipe in C. second ed. Cambridge: Cambridge University Press; 1992.
48. Pincus S. Approximate entropy (ApEn) as a complexity measure. Chaos 1995; 5(1): 110-117.
49. Parish LM, Worrell GA, Cranstoun SD. Long-range temporal correlation in epileptogenic and non-epileptogenic human hippocampus. Neuroscience 2004; 125(4): 1069-1076.

## Figures

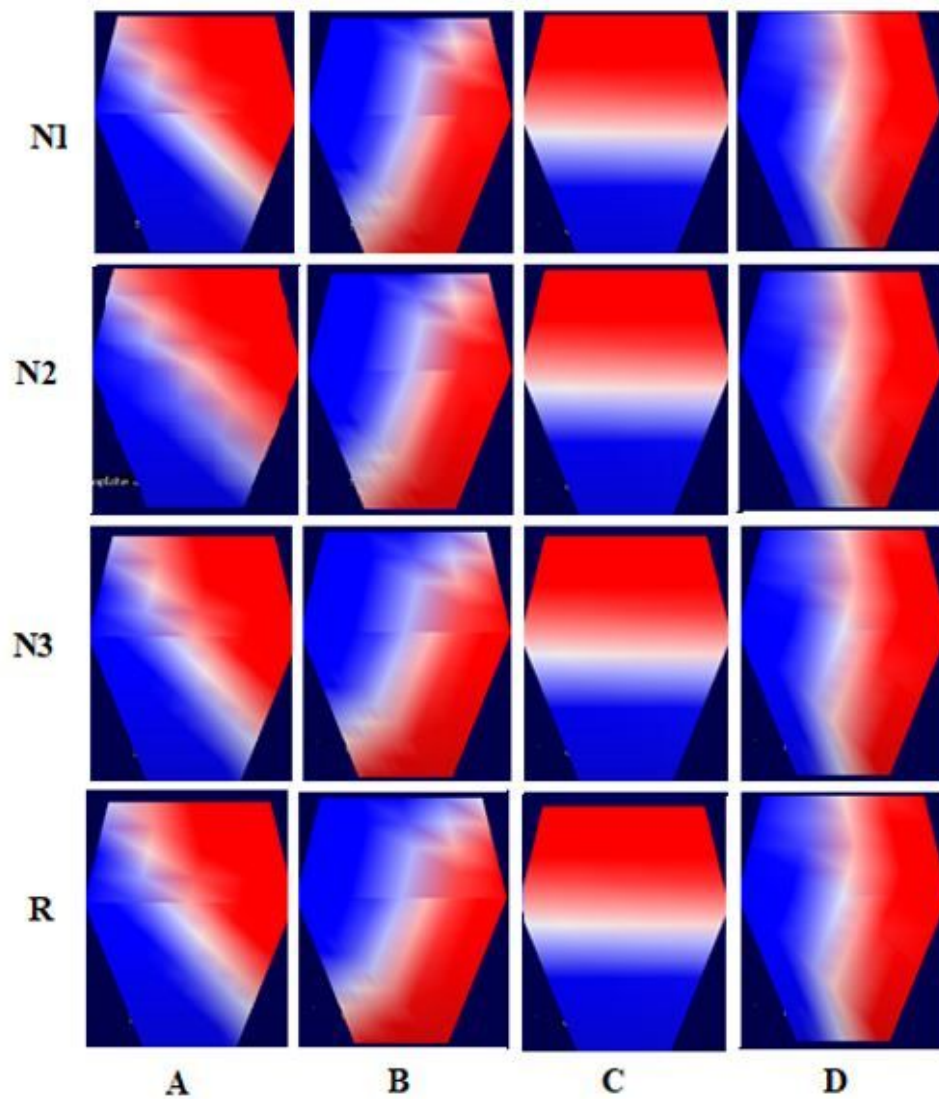


**Figure 1**

Microstates of normal W, N1, N2, N3 and R sleep stages. Healthy controls have four similar microstates A, B, C and D in four sleep stages.

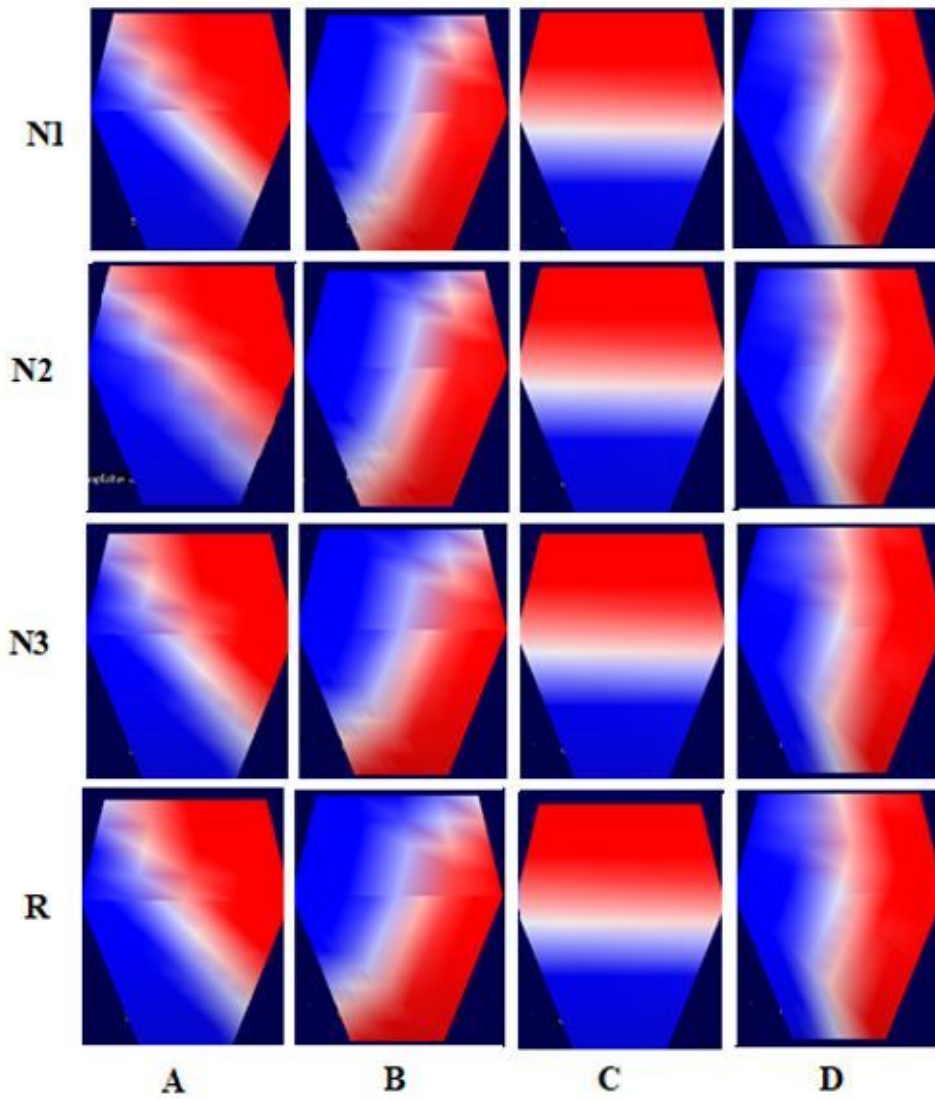


**Figure 1**

Microstates of normal W, N1, N2, N3 and R sleep stages. Healthy controls have four similar microstates A, B, C and D in four sleep stages.

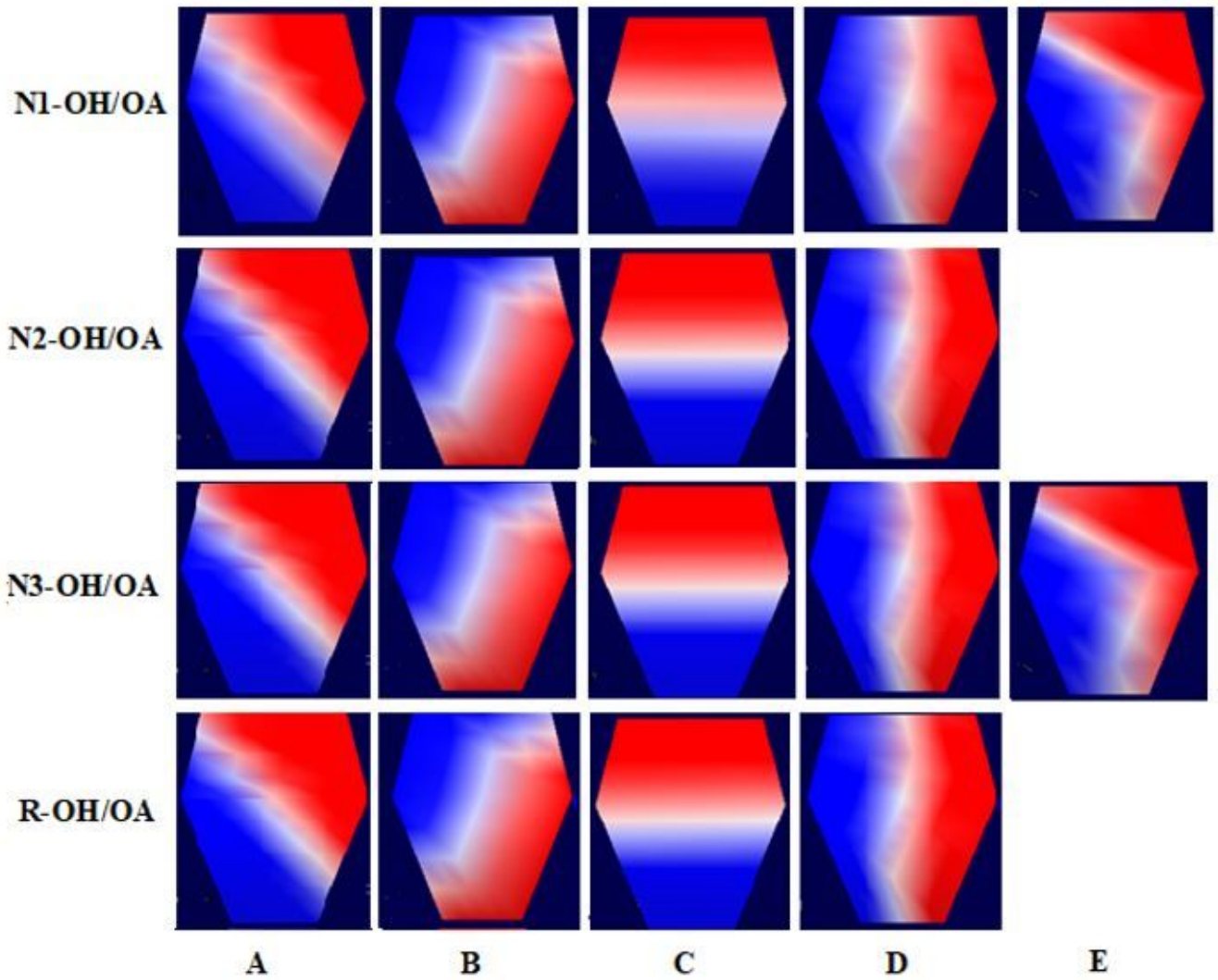


**Figure 2**

Microstates of OSA patients in sleep stages of N1-OH/OA, N2-OH/OA, N3-OH/OA, R-OH/OA. OSA patients have four microstates similar to healthy controls, but there is an additional microstate E in N1-OH/OA and N3-OH/OA stages.

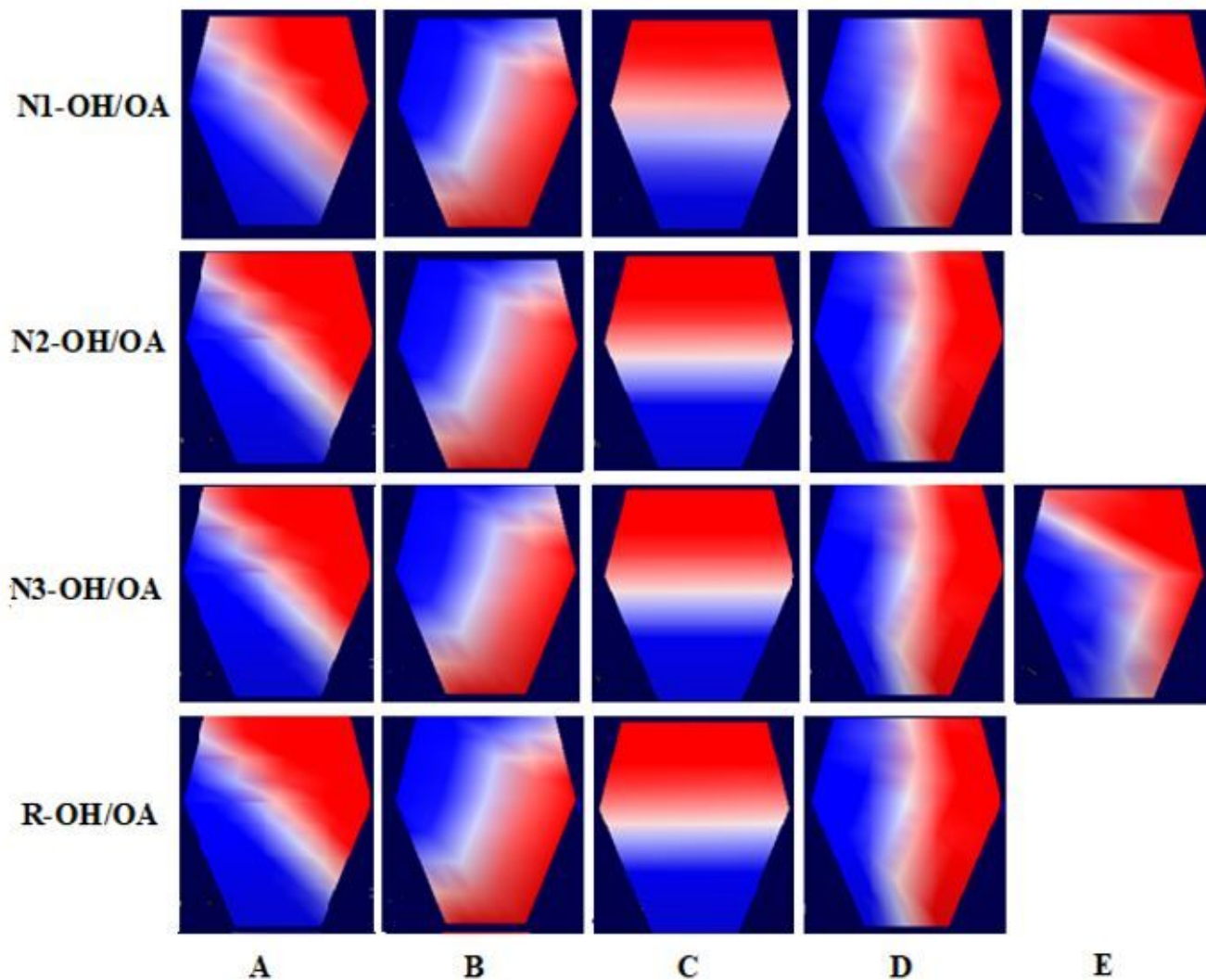


**Figure 2**

Microstates of OSA patients in sleep stages of N1-OH/OA, N2-OH/OA, N3-OH/OA, R-OH/OA. OSA patients have four microstates similar to healthy controls, but there is an additional microstate E in N1-OH/OA and N3-OH/OA stages.

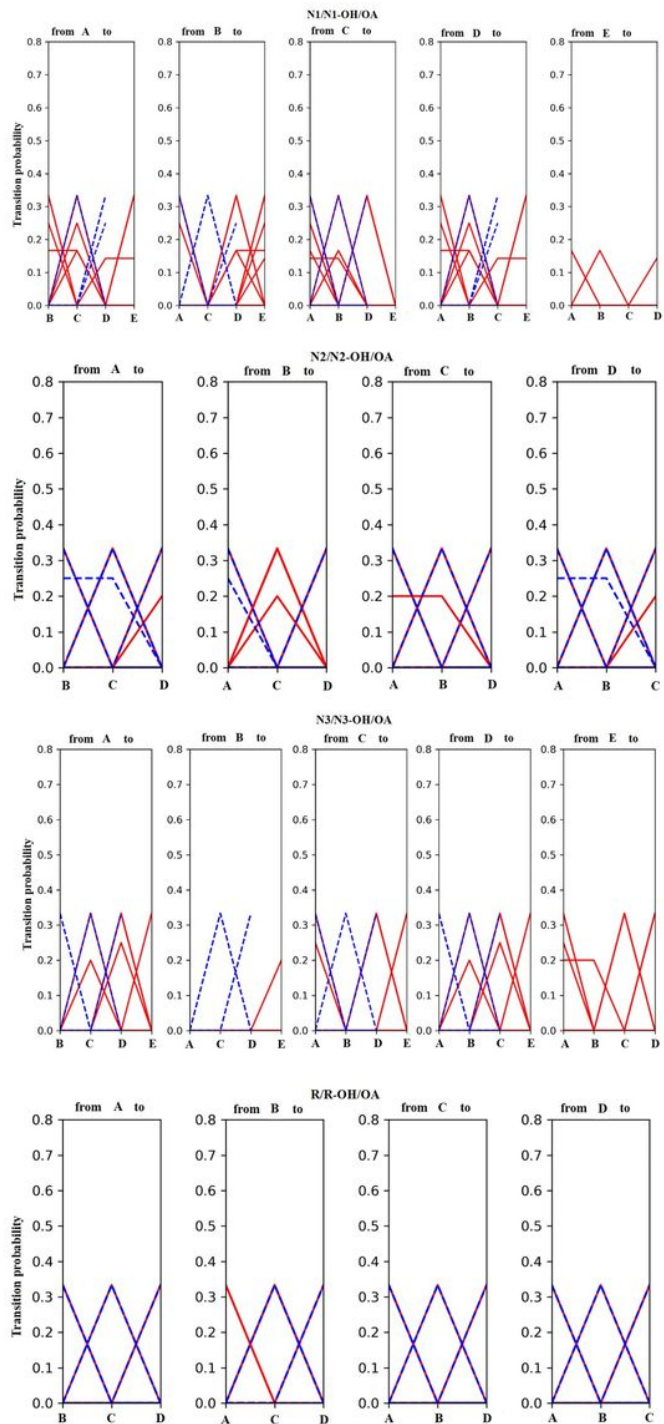


**Figure 3**

Transition probabilities (TPs) in two groups. For the maps given at the top of a column the transition probability to each of the maps at the bottom is given on the ordinate axis (healthy controls in blue for N1, N2, N3 and R stages, OSA patients in red for N1-OH/OA, N2-OH/OA, N3-OH/OA and R -OH/OA stages).

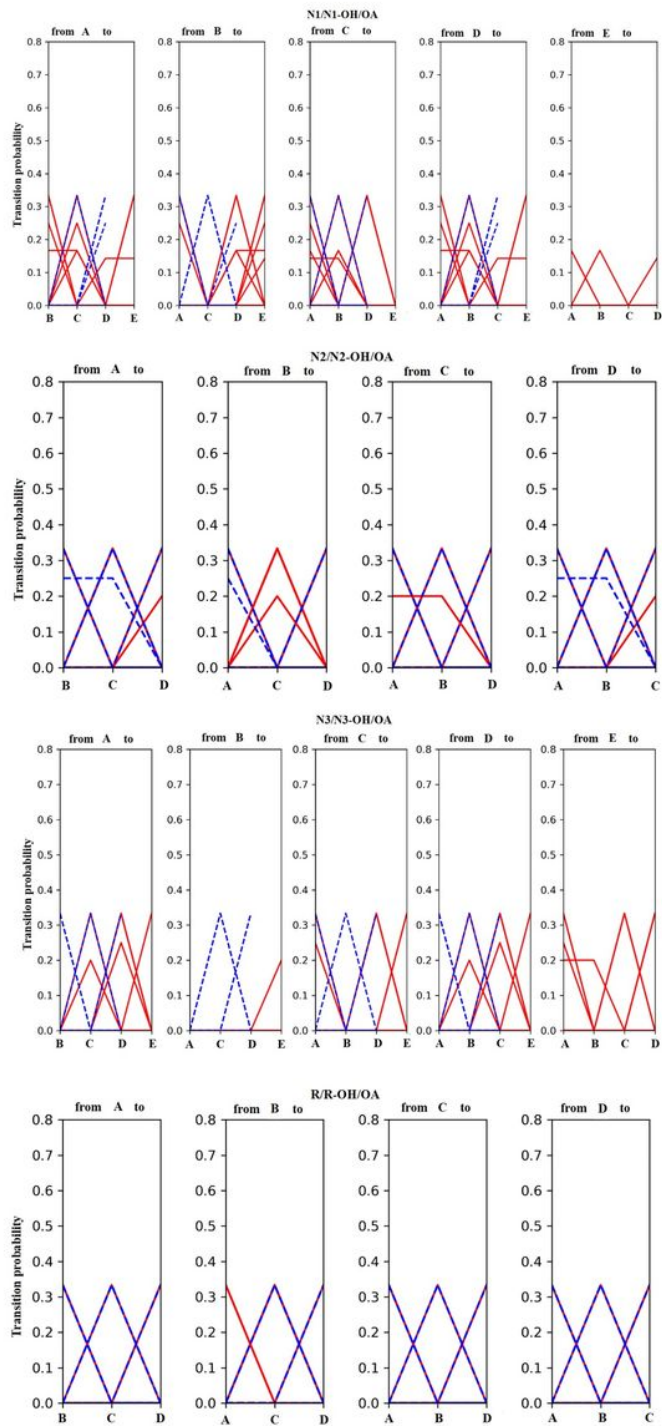


**Figure 3**

Transition probabilities (TPs) in two groups. For the maps given at the top of a column the transition probability to each of the maps at the bottom is given on the ordinate axis (healthy controls in blue for N1, N2, N3 and R stages, OSA patients in red for N1-OH/OA, N2-OH/OA, N3-OH/OA and R -OH/OA stages).

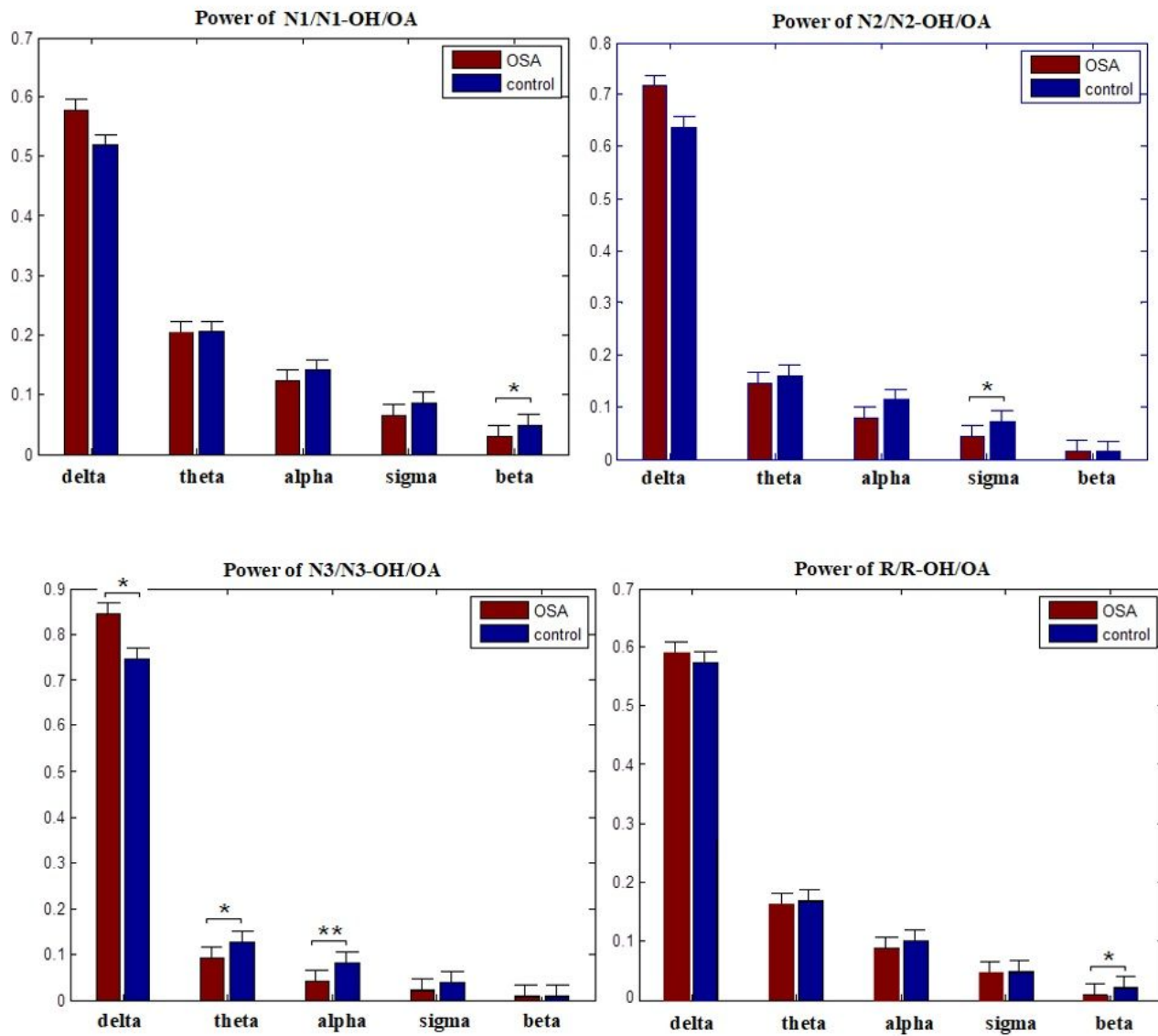


**Figure 4**

The power spectrum of two groups in the delta, theta, alpha, sigma and beta band in four sleep stages. Stars represent significant difference in five bands of two groups (Bonferroni corrected:  $P^* < 0.05$ ,  $P^{**} < 0.05$ ).

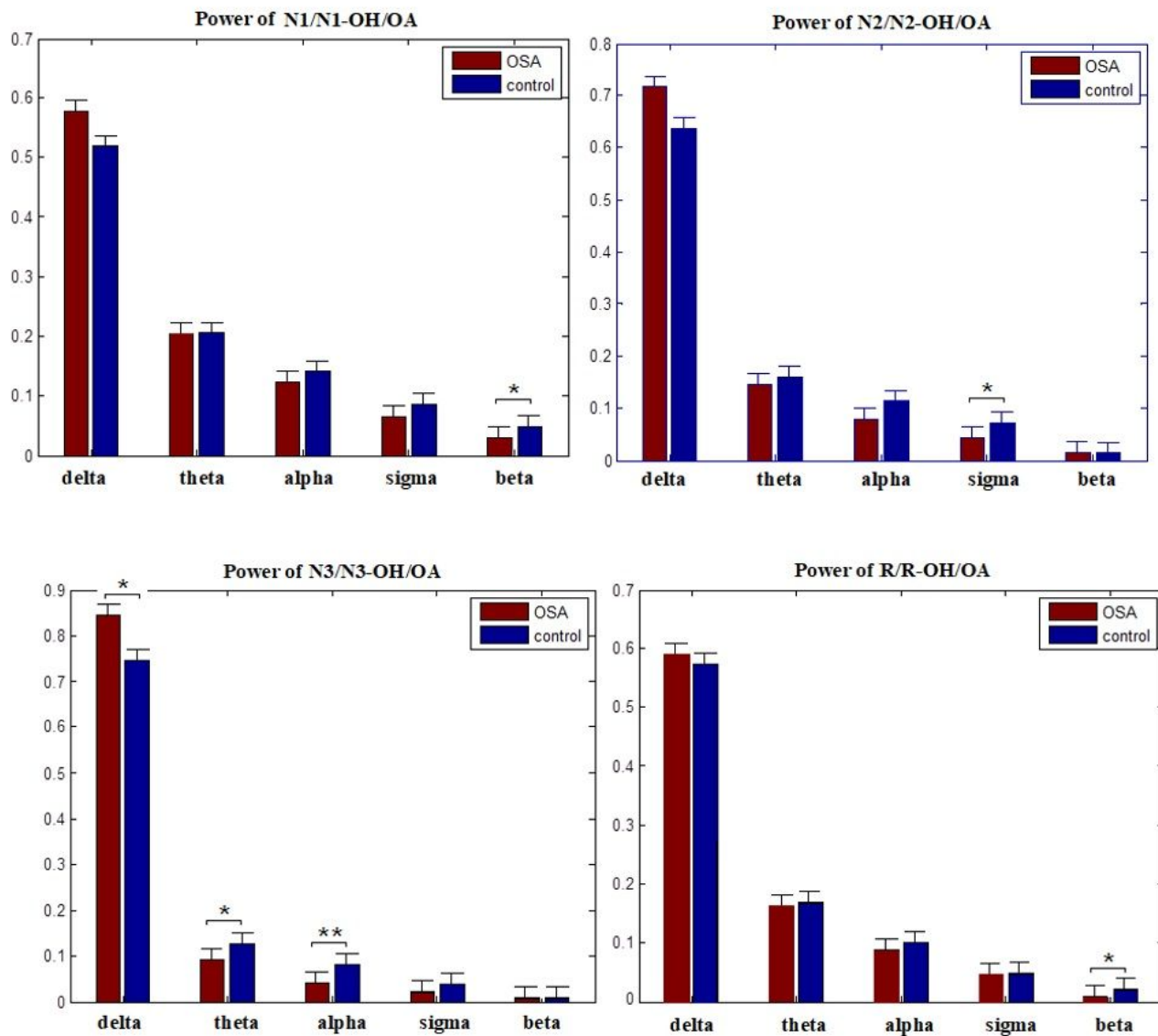
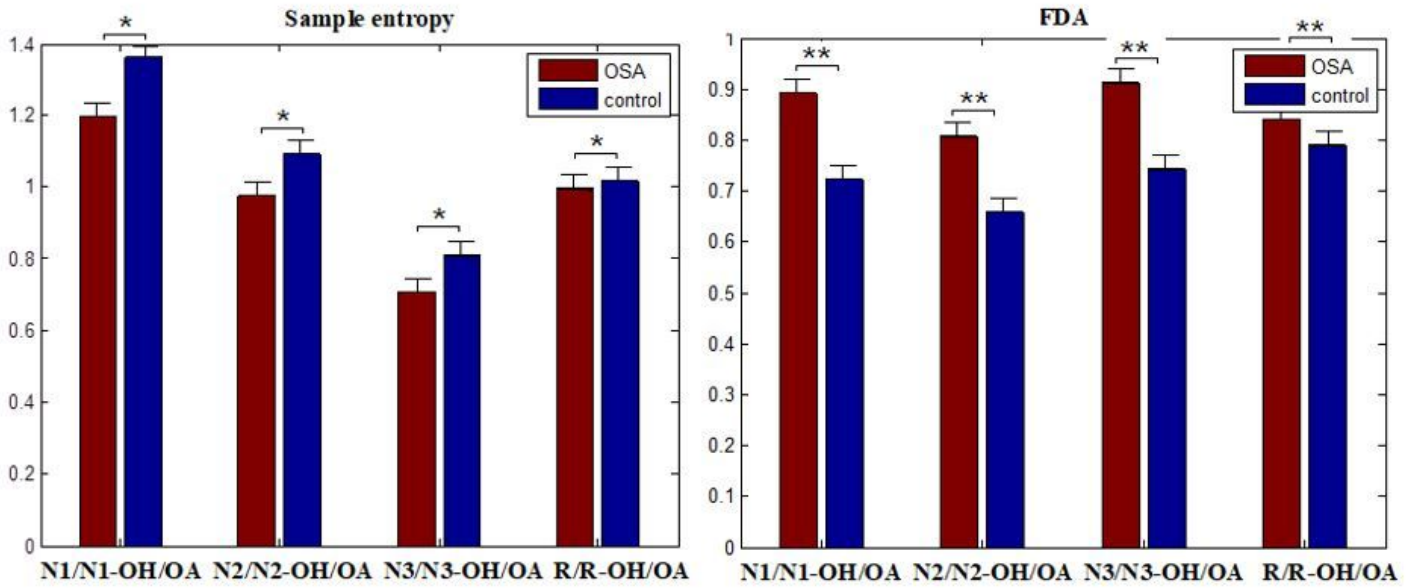


**Figure 4**

The power spectrum of two groups in the delta, theta, alpha, sigma and beta band in four sleep stages. Stars represent significant difference in five bands of two groups (Bonferroni corrected:  $P^* < 0.05$ ,  $P^{**} < 0.05$ ).

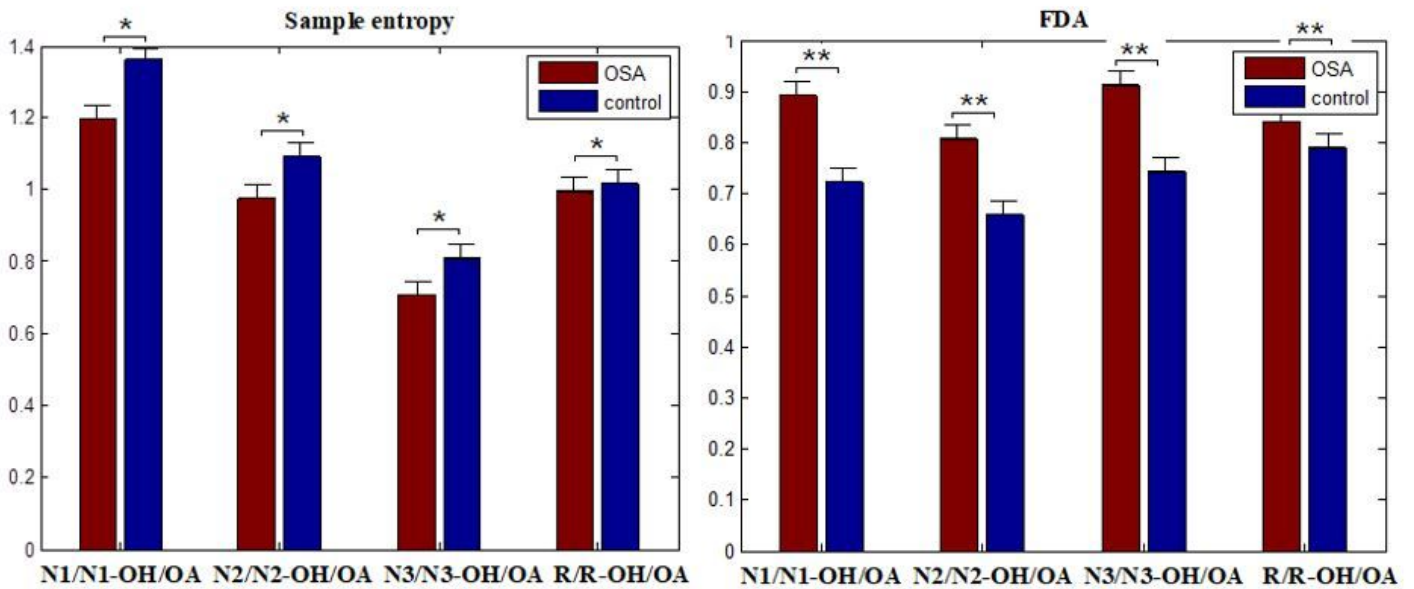


(a) Sample entropy

(b) Scale index  $\alpha$  of DFA

Figure 5

The sample entropy and scale index  $\alpha$  of two groups in four stages. In the NREM stage, the sample entropy of two groups from N1 to N2 to N3 decreases continuously, but increases in R phase. The sample entropy of OSA patients is lower than that of healthy controls. The scale index  $\alpha$  of OSA patients is higher than healthy controls in four sleep stages, and the scale index  $\alpha$  of OSA patients in N1-OH/OA and N3-OH/OA stages is higher than that in N2-OH/OA and R-OH/OA stages. Stars represent significant difference of two groups (Bonferroni corrected:  $P^* < 0.05$ ,  $P^{**} < 0.05$ ).



(a) Sample entropy

(b) Scale index  $\alpha$  of DFA

Figure 5

The sample entropy and scale index  $\alpha$  of two groups in four stages. In the NREM stage, the sample entropy of two groups from N1 to N2 to N3 decreases continuously, but increases in R phase. The sample entropy of OSA patients is lower than that of healthy controls. The scale index  $\alpha$  of OSA patients is higher than healthy controls in four sleep stages, and the scale index  $\alpha$  of OSA patients in N1-OH/OA and N3-OH/OA stages is higher than that in N2-OH/OA and R-OH/OA stages. Stars represent significant difference of two groups (Bonferroni corrected:  $P^* < 0.05$ ,  $P^{**} < 0.05$ ).

## Supplementary Files

This is a list of supplementary files associated with this preprint. Click to download.

- [AppendixA.docx](#)
- [AppendixA.docx](#)
- [AppendixB.docx](#)
- [AppendixB.docx](#)